



ELSEVIER

Journal of Applied Geophysics 37 (1997) 85–102

JOURNAL OF  
APPLIED  
GEOPHYSICS

## Study of the Chaves geothermal field using 3D resistivity modeling

Fernando Acácio Monteiro Santos<sup>\*</sup>, António Roque Andrade Afonso,  
Luís Alberto Mendes Victor

*Departamento de Física da Faculdade de Ciências da Universidade de Lisboa, Centro de Geofísica da Universidade de Lisboa, Rua da Escola Politécnica, 58-1250 Lisbon, Portugal*

Received 4 April 1996; accepted 12 March 1997

### Abstract

The present paper deals with the 3D modeling of a resistivity data set, carried out over the Chaves graben where the hot springs, with a temperature reaching 78°C, have a great economic importance. The main objective of the modeling was to incorporate the partial knowledge obtained from previous 1D and 2D interpretations into a three dimensional model. The 3D models of three rectangles and two dipole–dipole surveys, which were performed to detect conductive zones associated with the hydrothermal circulation, depict the general form of the graben and the spatial configuration of the low resistivity zones (10–15  $\Omega$  m). The achieved models exhibit several characteristics similar to those of previous 1D and 2D interpretations and are consistent with geological information and new findings related to the bed-rock depth (1200 to 1500 m), the northern and southern borders of the conductive zones and its connection with the fault systems.

*Keywords:* applied geophysics; DC resistivity; three-dimensional modeling; geothermics; Chaves graben

### 1. Introduction

Between 1990 and 1993 geophysical, geological and geochemical research were performed in the Chaves region (NE Portugal) to construct the hydrothermal model associated with the known hot springs. A hydrothermal field, where the hot waters reach a temperature of 78°C, is known at least since Roman times. The hot waters are used for medical purposes and are of good economical potential for the region. The waters belong to the bicarbonate/

sodium/CO<sub>2</sub>-rich type and the relatively high Cl content ( $\approx$  45 mg/l) indicates that the geothermal reservoir is liquid rather than vapor dominant (Aires-Barros et al., 1994).

Various geophysical methods, mainly gravity, resistivity, self-potential, scalar audio-magnetotelluric and magnetotelluric (MT), have been used to examine the shallow and deep structures of the Chaves graben. Based on these studies, the construction of a preliminary hot water circulation model was made possible. The meteoric origin and the most probable recharge area, situated at the north-east of the graben, have been inferred from the geochemical and isotopic studies (Aires-Barros et al., 1994). The MT

<sup>\*</sup> Corresponding author. Fax: +351-1-3953327; e-mail: fraissa@skull.cc.fc.ul.pt.

results provided a structural model of the area, where two principal fault systems ( $N65 \pm 10E$  and N–S) seem to control the deep circulation and upward flow of the hot fluids (Monteiro Santos et al., 1995a). The resistivity and audio-magnetotelluric surveys (Andrade Afonso et al., 1994; Monteiro Santos et al., 1996), were able to provide information about the geoelectrical structures of the graben. The question is whether, under conditions of strong lateral heterogeneity, 1D and 2D interpretations may be used to infer a realistic resistivity depth model. In an attempt to solve these questions we have performed a 3D interpretation which provides constraints on geoelectrical parameters and on geological structures of the Chaves graben.

In the last two decades a lot of efforts have been made in order to develop three-dimensional resistivity modeling algorithms using a finite-difference approach (Scriba, 1981; Dey

and Morrison, 1979), finite-element methods (Pridmore, 1978) and an integral equation (Raiche, 1974; Bakbak, 1977; Poirmeur and Vasseur, 1988). However, 3D interpretation of actual cases is not common in the literature. In this paper we present the results of the 3D modeling of the resistivity data carried out in the Chaves depression. The paper begins with a brief discussion of some previous geophysical results, in order to establish the practical limits of the 1D and 2D interpretation and to give some constraints on the 3D model. The 3D modeling procedure is then described and the results are discussed.

## 2. Geological setting

The studied region is dominated by the Chaves sedimentary basin (Quaternary), a

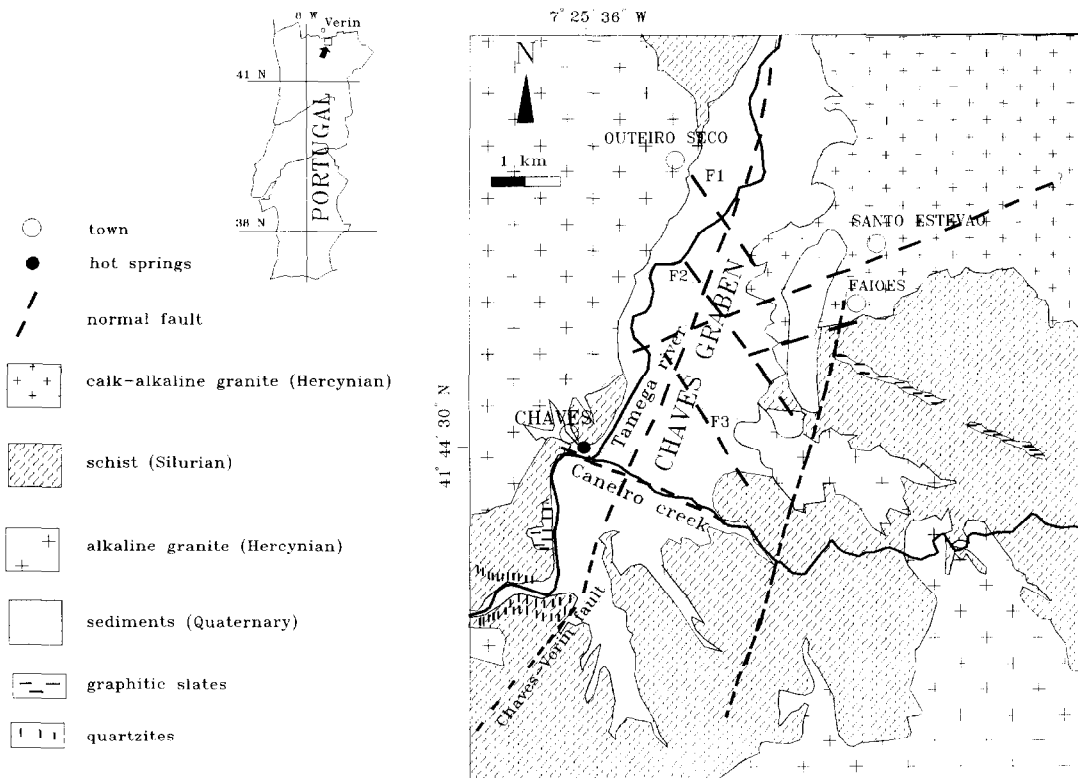


Fig. 1. Geological sketch map of Chaves region (adapted from Geological map No. 6-B of the Serviços Geológicos de Portugal).

graben whose axis has a NNE–SSW direction, bound by the granitic (Hercynian) and metamorphic schistose formations (Fig. 1). Northwards, the depression extends through the Verin basin (Galiza), similar to the Chaves one.

The oldest formation in the region (ante-

Ordovician) is represented by the schist–graywacke complex. Later, on the Ordovician–Silurian, quartzites and schists were formed. They have been metamorphosed by the Hercynian granitic intrusions, at the end of the Paleozoic. Mixed with the schistose complex, there

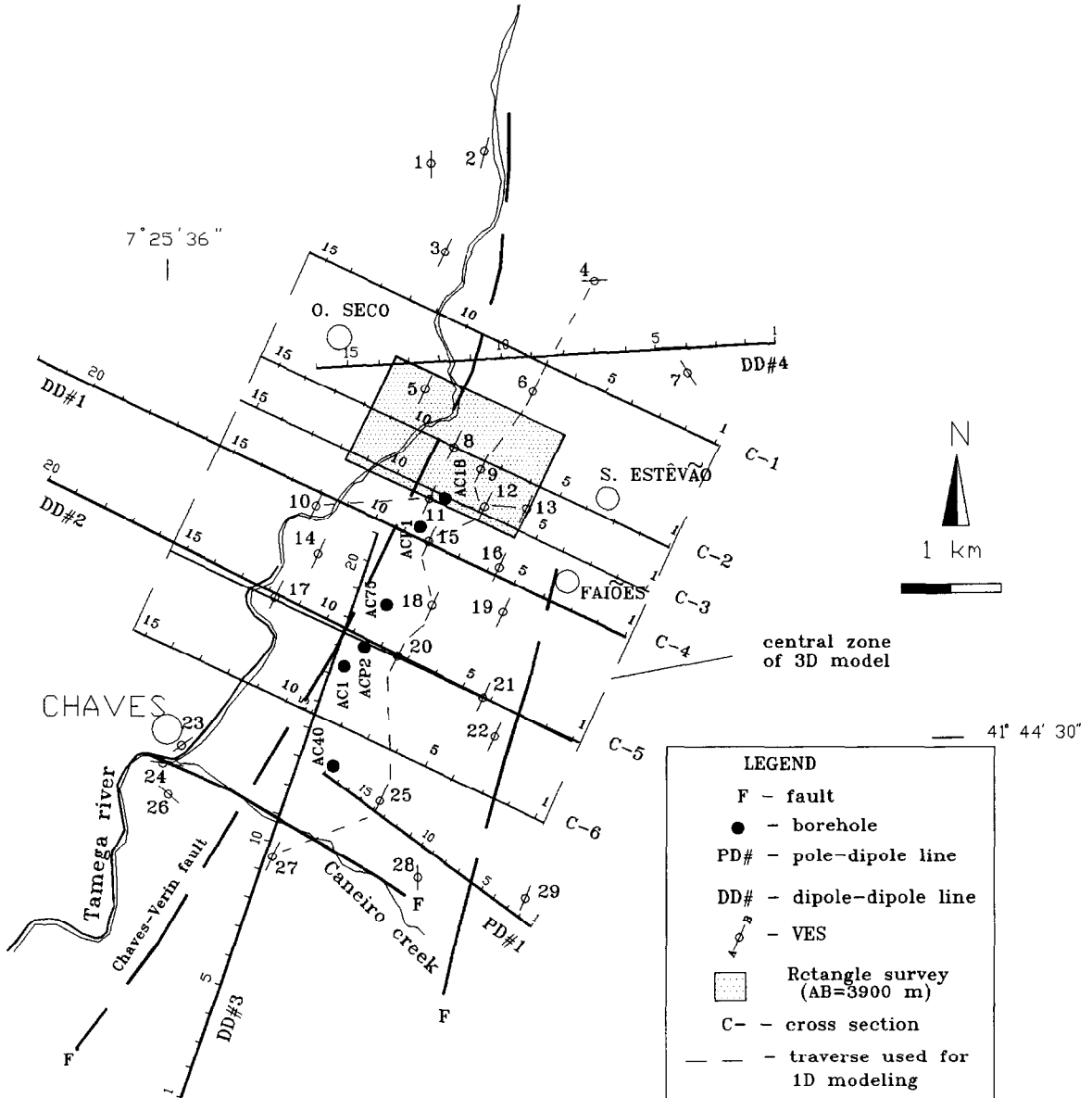


Fig. 2. Location of the surveys. The center of the VES is indicated by a circle and the direction of the expansion is indicated by a line.

are bands of graphitic slates, mainly in the southern part of Chaves town and south-east of Faiões.

The Alpine orogeny was the main cause of extensive tectonic activities and it was responsible for the formation of the hydrothermal field. The Chaves graben was formed by the relative motion of the blocks with different types of sediments being settled. The most recent formations are a sedimentary series (lacustrine, alluvial, colluvial, detritic, etc.) with variable thickness that had their origin during the Miocene (Universidade de Trás-os-Montes e Alto Douro, 1992). Two main faults play an important role: the NNE–SSW Chaves–Verin fault and the N70–80E fault system crossing the area in the neighbourhood of Faiões and S. Estêvão. The NNE–SSW fault corresponds to a tardi-Hercynian tectonic episode (280–300 My). According to a MT impedance tensor analysis, the deep direction of that incident is almost N–S (Monteiro Santos et al., 1995a). Intense neotectonic activity has reactivated the old fractures, originating a complex pattern of faults in the sedimentary basin. The present regional tectonic stress field, where the maximum horizontal compressive stress trends NW–SE to WNW–ESE (Universidade de Trás-os-Montes e Alto Douro, 1992), favours the ascent of geofluid at the crossing of the NNE–SSW, NNW–SSE and N70–80E faults.

### 3. Geophysical data and previous interpretation

The geoelectrical method has been applied to detect and define the geometry of the shallow hot water circulation zones within the graben. The survey comprised 29 Schlumberger vertical electrical soundings (VES), dipole–dipole lines, pole–dipole lines and rectangle surveys (Fig. 2).

#### 3.1. The schlumberger VES

The majority of the VES were made with AB electrodes expanding in the NNE–SSW direc-

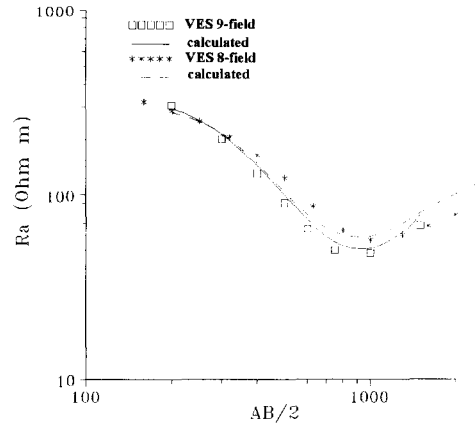


Fig. 3. Curves of apparent resistivity (Schlumberger) for the VES 8 (stars) and VES 9 (squares) soundings. Dashed and solid lines, are 3D model responses.

tion and with a maximum electrode spacing ( $AB/2$ ) ranging from 1200 to 2000 m. Exceptions to this are a few soundings carried out over syn-tectonic granite, with a maximum spacing between 150 and 500 m. The soundings may be divided into two main classes, corresponding to different electrical and geological sections. The first group of soundings comprising of curves of type QQH and HQH, were made in the eastern and central part of the graben, respectively, where the sedimentary sequences are thick. Fig. 3 shows two typical apparent resistivity curves of this group. The second group of soundings is comprised of curves of type QH obtained in areas where the bedrock is very shallow, i.e. mainly in the western part of the graben.

Previous interpretation of the resistivity data set was performed by Andrade Afonso et al. (1994). The data acquired within the graben, were inverted assuming layered models, the main features being:

- the sedimentary upper layers (Pleistocene) with a total thickness ranging from 100 to 300 m have resistivities in the 100–750  $\Omega$  m range;
- the intermediate conductive layer (11–25  $\Omega$  m) has a thickness ranging from 200 to 500 m; this layer has been associated with the geothermal reservoir;

— the bedrock, from 400 m to a greater depth is heterogeneous with the resistivity varying according to the nature of the geological formations (schistose or granitic) in the range 120–770  $\Omega$  m.

The geoelectrical parameters related to the uppermost layers are quite well resolved, but only the conductance of the low resistivity layer is well resolved; moreover, the basement resistivity and depth are usually poorly resolved.

The inversion results of some soundings were combined to obtain a resistivity cross section (profile) as displayed in Fig. 4. The VES 18 requires the introduction of a layer more resistive than the rest of the profile, indicating either the presence of a minor horst southernmost of the main intrusion of granite (beneath VES 12 and VES 15) or a high resistivity overburden. The profile shows a very large conductive zone dipping towards the central part of the basin. The variation in the bed-rock resistivity may

indicate the geological difference in the basement: granite towards the north and schist towards the south.

The most important features of the E–W cross section (Fig. 4 bottom) are the large depth of the basement beneath the VES 11, which corresponds to the Chaves–Verin fault, and the variation in the resistivity values (from 35 to 190 m), between VES 11 and VES 10, associated with the sedimentary and the presence of near surface granitic altered formation, respectively.

### 3.2. Drill information

There are many shallow wells in the basin drilled in the frame of a fresh water research project (Hidroprojecto, 1987). The locations of the most important drills are shown in Figs. 2 and 4 (top). On this figure the lithological correlations corresponding to Pliocene and Miocene

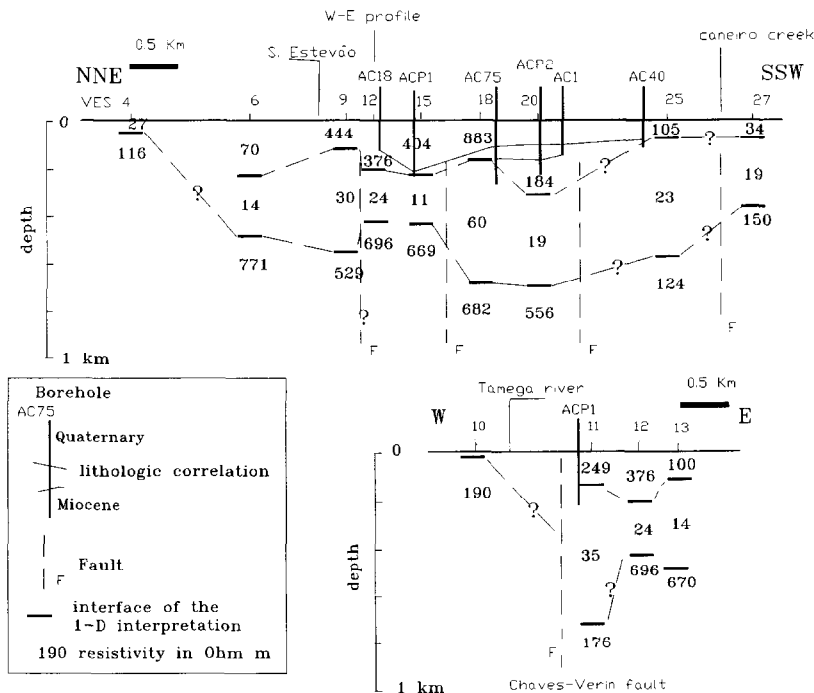


Fig. 4. Resistivity 1D sections along N–S (top) and E–W (bottom) directions. Also represented are the lithologic correlation given by solid lines (see Fig. 5).

units are represented by solid lines. None of the boreholes drilled in the depression reaches the schistose or granitic basement. The maximum depth attained is 225 m in the AC75 well. In Fig. 5 the stratigraphic sketch from the deepest boreholes (ACP1 and AC75) are shown. The Quaternary overburden has a different thickness in both wells and the Miocene is not reached in the ACP1 well.

In Fig. 5 the one-dimensional resistivity inversion of VES 15 and the drill section from the ACP1 well are compared. The difference between the uppermost geoelectric model and the geological section can be explained by the proximity of the road to Spain, which biased the resistivity data. The argillite formation is marked by a conductivity increase at a depth of 220 m (ACP1 well). Comparing the 1D resistivity models and the borehole data (Fig. 4 top) we can assume that the low resistivity layer corresponds to the Miocene units. However, the depth and the resistivity of the basement are not well defined, probably due to the 3D effects of the

complicated geoelectrical structure of the graben, which is ignored by the 1D methodology.

### 3.3. Dipole–dipole lines

In Fig. 6, the field pseudo-sections corresponding to four lines of dipole–dipole measurements (dipole length of 300 m) performed in the region are shown. Fig. 7 shows the field pseudo-section of a pole–dipole survey, performed in the southeastern part of the graben (PD#1). All the data were previously modeled using a trial-and-error procedure and with the assumption of a 2D approximation (Andrade Afonso et al., 1994). In Fig. 8 one such model is presented. The main characteristics of the dipole–dipole models obtained from DD#1 and DD#2 lines, are:

- an overburden with a thickness ranging from 250 to 300 m and an exhibited resistivity range of 100–400  $\Omega$  m;

- low resistivity zones (12–15  $\Omega$  m) in the central and eastern parts of the graben;

- an electrical basement at a depth not well defined (the smallest value is 1500 m in DD#2 profile), with a resistivity of 180 m. Towards the west, the conductive zone is bound by the well known Chaves–Verin fault. The resistivity of the bodies at the east edge of such models is poorly resolved due to the short length of the geoelectrical profiles.

The difference between the depth of the geoelectric basement obtained by dipole–dipole lines and the depth calculated from the VES models can be explained by the electrical macroanisotropy in relation with faults (Campbell, 1977). This includes the electrical (lithologic) heterogeneity and the geometric complexity of the medium, as well as the different approaches in the data interpretation (Appendix A). While the VES were interpreted by assuming a laterally large layered earth, the dipole–dipole lines were interpreted by assuming a two-dimensional medium. In Table 1 a comparison between geometrical and electrical parameters

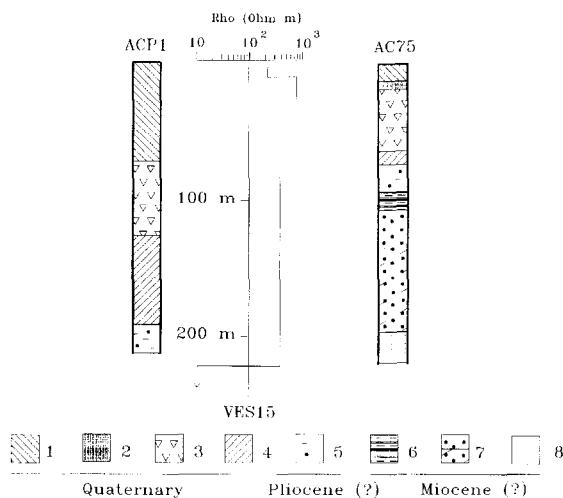


Fig. 5. Stratigraphy from the deepest boreholes in the graben and the 1D model from the VES15. Legends: 1, superficial gravel deposits; 2, clay; 3, unit with interlayered clays, sands and pebbles; 4, intermediate gravel deposit; 5, sandstone and arkoses; 6, argillite; 7, conglomerates and sandstones; 8, lower clay.

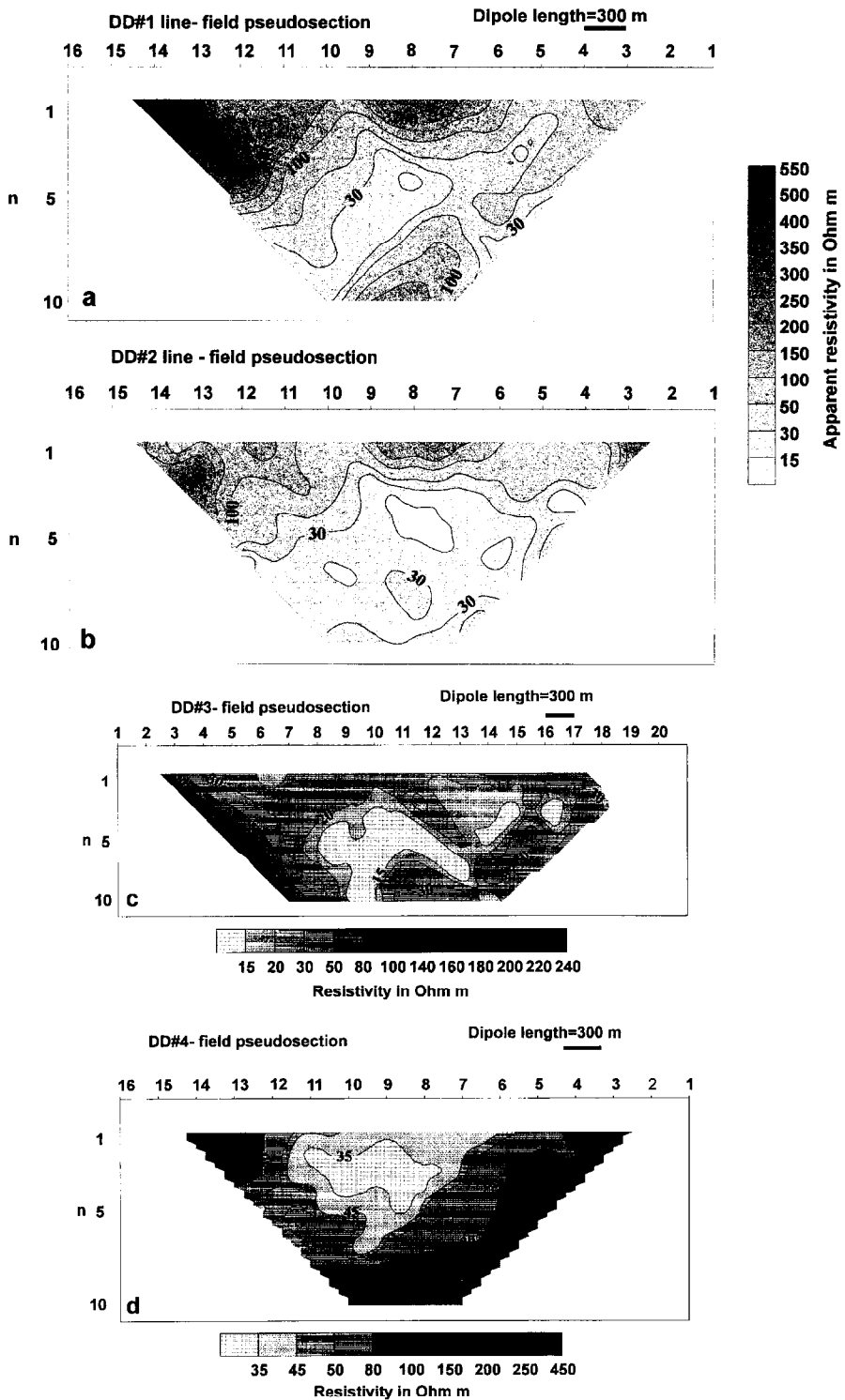


Fig. 6. Dipole–dipole apparent resistivity pseudosections (field): (a) DD#1, (b) DD#2, (c) DD#3 and (d) DD#4 lines.

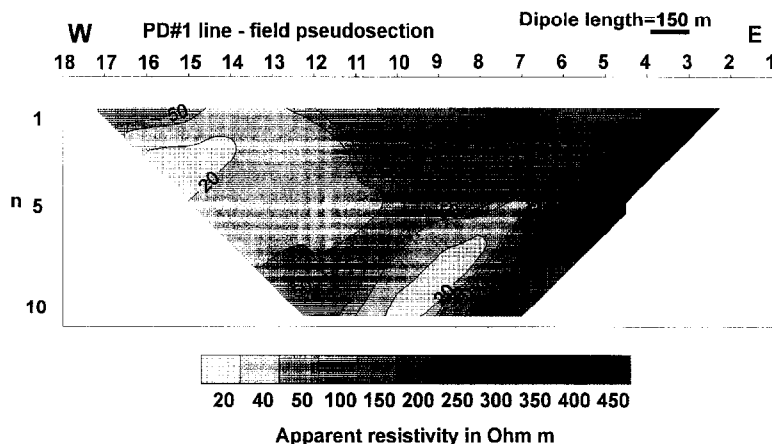


Fig. 7. Pole-dipole apparent resistivity pseudosection (field) from PD#1 line.

Table 1  
Comparison between geometrical and electrical parameters from VES and dipole-dipole modeling

Zone	Configuration	Thickness or depth (m)	Resistivity ( $\Omega$ m)
Overburden	DD#2	250	200
	VES20	310	184
Conductive zone	DD#2	1350	12
	VES20	388	19
Basement	DD#2	1600 (depth)	180
	VES20	698 (depth)	556

While modeling the presented dipole-dipole lines we assumed that there was no change in resistivity along the graben. In the present situation such representation should be considered with some caution because the Chaves graben displays 3D features, as pointed out by the 1D resistivity interpretation and MT data (Monteiro Santos et al., 1995b). Therefore, a more detailed model of the Chaves depression requires a three-dimensional interpretation.

obtained by VES and dipole-dipole modeling is shown, using the VES 20 central point of the crossing between the DD#2 line of Fig. 6(b), with the NS profile of Fig. 4.

### 3.4. Gravity data

A two-dimensional gravimetric profile along the DD#2 line was performed. From its interpretation (Moreira, personal communication),

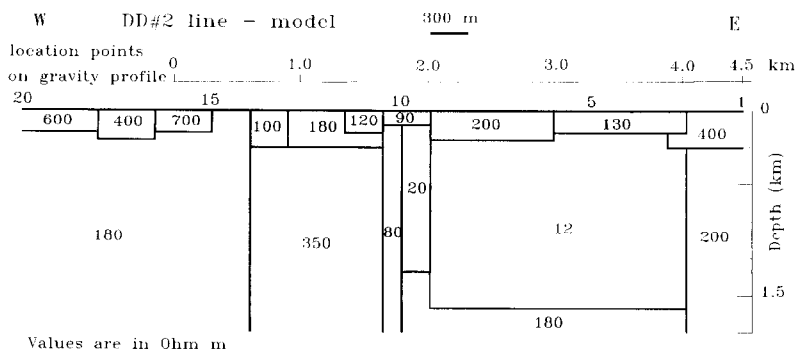


Fig. 8. Trial-and-error two-dimensional model from DD#2 dipole-dipole survey with indication of the gravity profile location of Fig. 9.

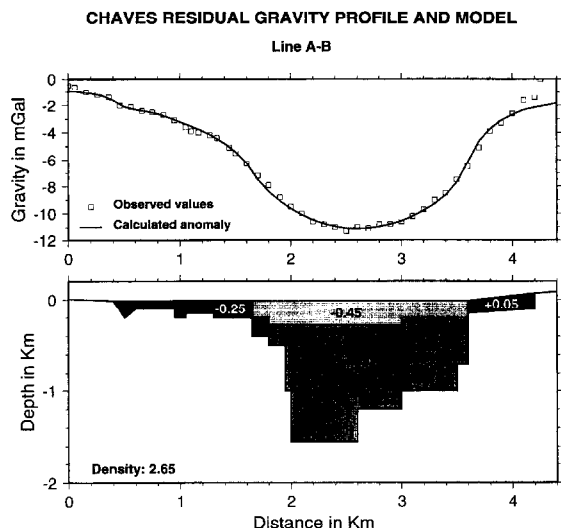


Fig. 9. Two-dimensional interpretation of a gravity profile over the Chaves graben, illustrating how limits to depth extent can be obtained from gravity data. The profile is collinear with the DD#2 dipole–dipole survey.

the bottom of the basin reaches a depth of 1600 m in the neighbourhood of the Chaves–Verin fault (Fig. 9). The residual gravity anomaly is characterized by a wide asymmetrical minimum in the graben ( $-11$  mGal), corresponding to the filling of the depression. The density difference between the sedimentary basin and the basement rocks was assumed to be  $-0.30$  g/cm<sup>3</sup>, with a  $2.65$  g/cm<sup>3</sup> density for the latter. The bedrock depth estimated from gravity data is consistent with the dipole–dipole result (DD#2 line) and will be taken into account in the depth constraints for the 3D model.

### 3.5. Rectangle surveys

In Fig. 10, the apparent resistivity data corresponding to the rectangle surveys centered at VES 8 are shown. These surveys were performed with the current electrode (AB) oriented in the NNE–SSW direction with a separation of 1000, 2000 and 3900 m and a potential electrode separation (MN) of 100 m. Fig. 2 shows the area of the largest of these rectangles. This

data was acquired to detect the low resistivity zones west of Faiões and S. Estêvão.

## 4. 3D methodology

From 1D and 2D resistivity interpretations the major lithologic units of the Chaves basin can be characterized. Nevertheless some aspects are still uncertain:

- the boundary of the conductivity anomaly is still not clearly displayed;
- the bedrock depth and conductivity are still under discussion;
- the general configuration of the granite intrusion in the graben is not defined.

The goal of this paper is to propose a 3D modeling of three resistivity rectangles, centered at VES 8 and two dipole–dipole lines (DD#1 and DD#2) crossing the graben. The modeling of the data was done using a trial-and-error method using a finite-elements algorithm (Pridmore, 1978). With this method, the region of interest is discretized into prismatic cells using a 3D orthogonal mesh. The main mesh is enlarged into an extended mesh so that remote boundary conditions can be imposed i.e. the homogeneous Neumann condition at the earth–air interface and the asymptotic condition used by Dey and Morrison (1979) at the subsurface external model boundaries. This condition imposes the asymptotic  $1/r$  behavior of the potential at large distances from the source ( $r$ ) on the edging planes of the model. For each cell of the model a constant resistivity is assumed. To check the accuracy of the mesh, apparent resistivity values over a  $100 \Omega$  m homogeneous half space were calculated. The results agree with the expected values to within 6%.

Because of the computer limitations and geophysical reasons, related to the orientation of the surveys, we divided the 3D model into two parts: (a) the northern one, that includes C-1 to C-3 cross-sections, which was performed using the rectangle data set and (b) the southern one, with C-4 to C-6 cross-sections, constructed us-

ing the dipole–dipole data. For the rectangular model, the half-space was discretized into  $47 \times 39 \times 16$  blocks (in N–S, E–W and vertical directions) and for the dipole–dipole model, into  $46 \times 64 \times 13$  blocks (in N–S, E–W and vertical directions). The computations were performed with an IBM-Risc/6000 workstation.

## 5. Results and discussion

### 5.1. The northern model

The general shape of the rectangle apparent resistivity data (Fig. 10), indicates an increasing conductivity with depth and also in a region that

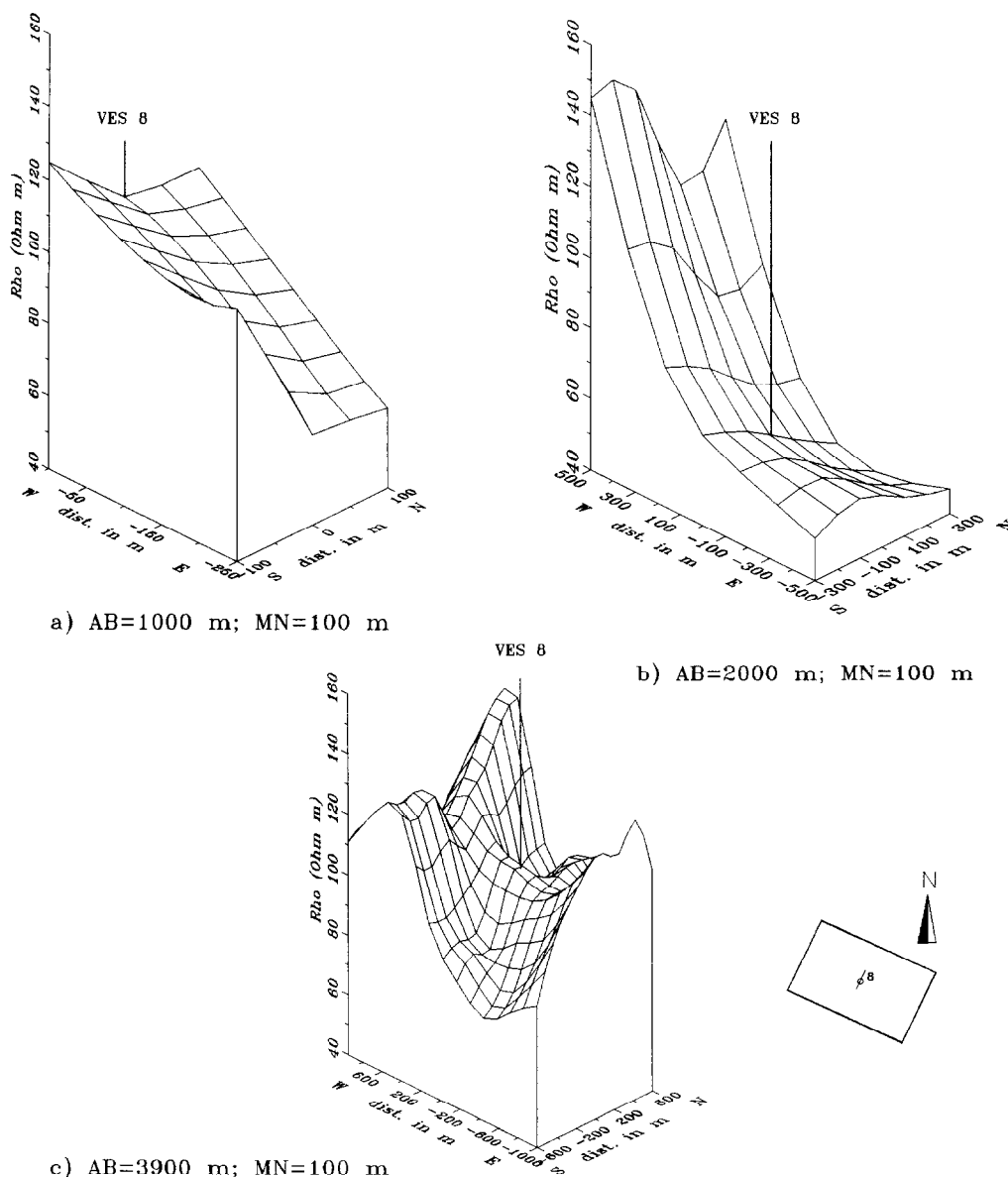


Fig. 10. Maps of experimental apparent resistivity for the rectangle surveys centered at VES 8 sounding.

trends towards N–S. Below the central point of VES 8, the conductivity increases with depth in the zone associated to  $AB/2 = 500$  m through 1000 m but it decreases from  $AB/2 = 1000$  m through 1950 m. Northwards this low resistivity zone was detected by the DD#4 line (Fig. 6(d)), beneath poles 10 to 12. In the third rectangle ( $AB = 3900$  m), the configuration of the apparent resistivity map indicates a NW–SE less resistive structure superimposed on a N–S striking one.

The trial-and-error model obtained from the rectangles (Fig. 11(a) top and (b) left) shows the location of the Chaves–Verin fault (C–V fault) and the geometry of a narrow low resistivity buried body (15 m). From the 3D model the bottom of the conductive body in the fault zone is defined at a depth close to 1500 m and dips to the south.

The more resistive area eastern to the Chaves–Verin fault ( $400 \Omega$  m), is interpreted as a granitic intrusion. The southern limit of this granitic block is a fault, trending N20–30W, extending westwards and it seems to be the limit of the granitic formation in the graben (fault F1 in Fig. 1). From the model the limit must be localized northwards of the position suggested from the 1D interpretation (Fig. 4 top).

The 3D model shows evidence of the smaller scale graben (the body of  $30 \Omega$  m and  $25 \Omega$  m, in the Fig. 11(a) westwards of S. Estêvão and Faiões), suggested by the interpretation of the VES data in this area (Andrade Afonso et al., 1994). Its geological structure seems to be well correlated to the NNE–SSW normal faults in the eastern part of the depression (Fig. 1).

The upper limits of the conductive body, in the survey area, are verified basically from the VES results. The comparison between the 3D model response and experimental data for the soundings VES 8 and VES 9 is illustrated in Fig. 3. In Fig. 12 the computed rectangle response calculated for the 3D model is shown. A comparison with Fig. 10 shows qualitatively that the model results fit quite well to the

observed data set. A statistical comparison gives values for the mean residuals and standard deviations (s.d.) of these residuals as follows: for  $AB = 1000$  m, a mean of 1.4 and a s.d. of 27; for  $AB = 2000$  m, a mean of 11 and a s.d. of 34 and for  $AB = 3900$  m, a mean of 5 and a s.d. of 21.

## 5.2. The southern model

The two field dipole–dipole pseudosections (DD#1 and DD#2) show a region of low apparent resistivity corresponding to the graben fill and hydrothermal circulation, in the same direction as the low apparent resistivity of the rectangle. The anomaly patterns in the pseudosection of those dipole–dipole lines are very similar. Considering the distance between the profiles ( $\approx 1.2$  km) these anomalies represent a fairly large conductive structure.

In the 3D model obtained from the dipole–dipole surveys (Fig. 11(a) bottom and (b) right), low resistivity zones ( $10 \Omega$  m) are well displayed in the central and eastern zones of the graben. The basement ( $150 \Omega$  m) lies at a depth that varies between 1200 and 1600 m. The Chaves–Verin fault, corresponding to a sharp lateral discontinuity is well displayed.

The SE zone of the 3D model is constructed according to the data of the PD#1 line, which reveals a low resistivity area interpreted as being due to a hot water flow (beneath poles 14 to 16 in Fig. 7). The complete resistivity survey (Andrade Afonso et al., 1994) of the Chaves region, demonstrates the existence of an impermeable barrier (in the neighbourhood of the Caneiro creek and associated with the N40–50W fault) which compels the flow to circulate towards the Chaves hot springs. The barrier is confirmed by 2D interpretation of the DD#3 line, in the neighbourhood of poles 9 to 11 (Fig. 6(c)). The southern limit of the  $10 \Omega$  m conductive structure, in depth, could probably be due to a horst, as it was inferred from the geological information and the PD#1 survey.

A low resistivity zone towards the Chaves

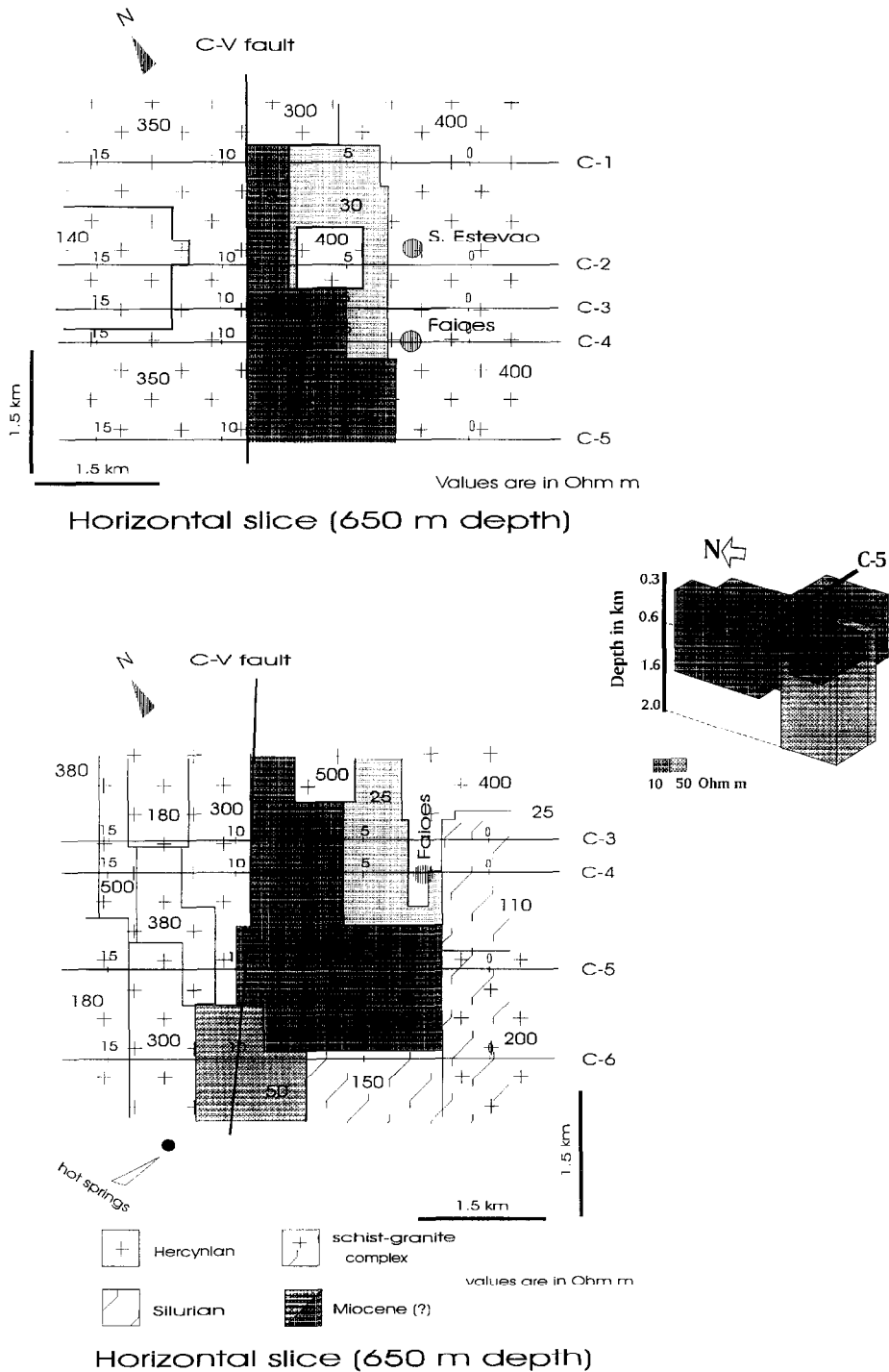


Fig. 11. (a) Horizontal slices (depth 650 m) of the three-dimensional resistivity model in the northern (top) and in the southern areas (bottom) of the graben. Also shown is a three-dimensional perspective of the low resistivity zones in the central part of the graben. (b) Cross sections of the three-dimensional resistivity models.



Fig. 11 (continued).

geothermal pole is shown in the SW part of the model (Fig. 11(a) bottom) according to the DD#3 survey. In fact, the DD#3 pseudosection presents a low resistivity anomaly (poles 12 to 15) which seems to be associated with a structure shallower than the one detected by the DD#1 and DD#2 surveys. This corresponds to the existence of fractures with shallow hot water circulation (Universidade de Trás-os-Montes e Alto Douro, 1992).

From the three-dimensional model, it can be seen that the low resistivity zones are connected to the N70–80E and N20–30W trending fault systems (Fig. 11). Due to their low resistivity,

such formations probably correspond to reservoirs filled with high mineralization hot fluid. In fact, the preliminary processing of temperature measurements, carried out in boreholes located in the graben, indicates that the geothermal gradient is of the order of 60°C/km. The estimated mean temperature in the aquifer lies between 52 and 62°C and at the deepest part of the aquifer the temperature values are near 100°C (Rosa Duque, personal communication).

It is known that the resistivity does not present typical values for each geological unit, but only ranges of values, into which different formations may be included. It follows that the

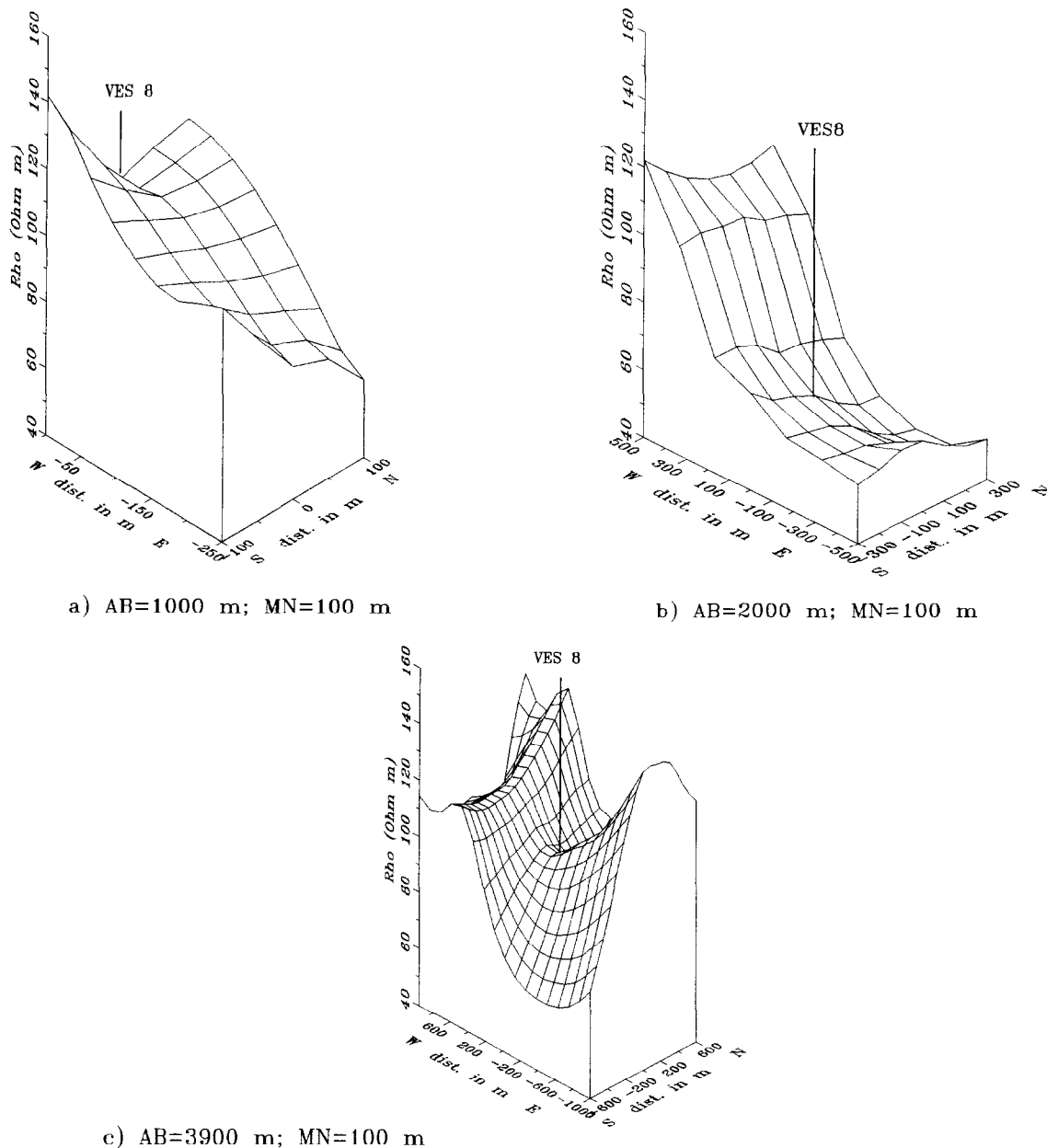


Fig. 12. Synthetic maps of apparent resistivity for the rectangle surveys.

interpretation in terms of lithology is ambiguous. The lithological nature of the basement may be discussed in two ways: the first is based on geological considerations and the second is based on the resistivity values measured on the surface.

According to the first view a granitic north-

ern bed-rock and a metamorphic (schistose complex) southern basement can be forecasted (Fig. 1). For the second view, let us consider the resistivity values obtained from audio-magneto-telluric soundings carried out on schistose formations (Monteiro Santos et al., 1996). They revealed a layer with resistivity between 115

and 140  $\Omega$  m and a thickness > 700 m, under a more resistive surface layer (with thickness ranging from 70 to 200 m and resistivity in the 400–800  $\Omega$  m range). The equivalent resistivity of these two layers does not reach 200  $\Omega$  m. Although this value is not as high as those commonly found on metamorphic rocks the presence of these formations in the underground graben regions is easily acceptable considering the water content and the temperature effects on the resistivity of the ionic solution.

A sensitivity test was performed by increasing or decreasing the resistivity of the basement of the model up to 300  $\Omega$  m or down to 75  $\Omega$  m, but the dipole–dipole response of these models did not fit the observed data as well as the models with the bed-rock resistivity at 150  $\Omega$  m. Although not well defined, the basement resistivity lies in the 100–200  $\Omega$  m range. Furthermore, checking on the validity of the models, the pseudosections of the observed and computed apparent resistivity (Fig. 13) fit satis-

factorily on a semi-qualitative basis. A statistical comparison gives the mean and standard deviation of these residuals as 9 and 46 for the DD#1 line and 4 and 23 for the DD#2 line, respectively.

The comparison between the calculated and observed apparent resistivity values for several soundings (AB = 2000 m) is given in Table 2. The values obtained from the northern-model agree quite well (with a maximum error of 28%) with the experimental ones. From the southern-model, the calculated and observed values show an almost constant relationship that is close to the macroanisotropy coefficient, the estimated value of this coefficient for the conductive body is  $\lambda = \sqrt{\rho_t/\rho_1} \approx 1.3$  (where  $\rho_t = 25 \Omega$  m is taken from averaging on VES soundings and  $\rho_1 = 15 \Omega$  m is taken from dipole–dipole surveys). A significant exception is the VES 22, located on the eastern part of the graben. This sounding was carried out over a granite outcrop, which affected the whole ap-

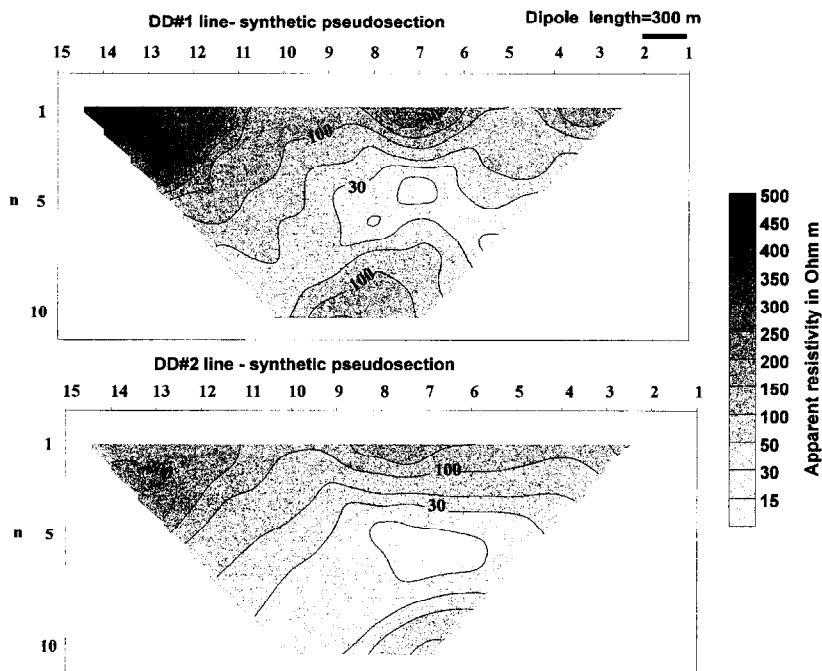


Fig. 13. Dipole–dipole apparent resistivity pseudosections (synthetic), from: DD#1 (top) and DD#2 (bottom) surveys.

Table 2  
Experimental and calculated values of apparent resistivity at the central point of AB = 2000 m

VES $\rho_a$ ( $\Omega$ m) experimental		$\rho_a$ ( $\Omega$ m) calculated	$\sqrt{\frac{\rho_{\max}}{\rho_{\min}}}$
Northern model			
8	52	60	—
9	48	55	—
11	48	54	—
13	48	58	—
Southern model			
14	170	119	1.2
15	50	67	1.2
16	80	51	1.3
18	95	37	1.6
19	55	40	1.2
20	55	31	1.3
21	48	33	1.2
22	220	46	2.2

parent resistivity curve, increasing the values. The mesh used in the modeling was not fine enough to represent the formation, the calculated apparent resistivity values being lower than the field ones. In the analysis of Table 2 it must be noted that the southern model was constructed taking into account the interpretation of data acquired with arrays in the NW–SE direction, while the calculated VES were made in the NNE–SSW direction.

The results confirm that the 3D model is compatible with the broad features of the Chaves graben field data and that for a more detailed modeling the anisotropy must be considered.

## 6. Conclusions

The electrical methods used in this study are adequate for investigating geothermal anomalies such as that in northeastern Portugal. The results of a 3D interpretation of the rectangle and dipole–dipole data carried out in the Chaves geothermal field, which incorporate knowledge obtained from previous 1D and 2D interpreta-

tions, are realistic, complete and consistent with the observed geological features.

Resistivity models resulting from the 3D modeling have features consistent with those observed in previous interpretations (i.e. a low resistivity zone (10  $\Omega$  m) in the central part of the graben bounded by more resistive rocks) and provide new findings for the spatial configuration of the anomalous zones.

The 3D model defines the northern and southern boundaries of the geoelectrical anomaly and its thickness exhibits the relationship of the anomaly with the major fault systems. In the basin, the boundary between granite and schist is associated with the N20W–30W fault cutting across the Chaves–Verin fault.

The model confirms the previous interpretation of Andrade Afonso et al. (1994) and Monteiro Santos et al. (1995a) in that: (1) the areas of upward flow are probably linked with the intersecting faults trading N70E–80E, N20W–30W and NNE–SSW (mainly between poles 6 and 10 of the DD#1 line) (Fig. 11) and in that (2) the shallow circulation of water in the graben seems to be mainly conditioned by neotectonic faults. From the pattern of the conductive zones, an enlargement of the circulation zone and a subdivision of the flow in the southern part of the graben were inferred.

## Acknowledgements

Many people have participated in the laborious field measurements and we are grateful to: Rogério Mota, Inês Rio, Rita Nolasco, Rui Gonçalves, Joaquim Marques and Virgílio Futre. We thank J. Ribeiro and INMG for the gravity profile data, J. Pous for the synthetic VES data and C.A. Dias and G. Vasseur for their careful reviews and many helpful suggestions. The hospitality of the residents of the Chaves town was an important factor for the successful work. The field work of this research was financed by CE under the scope of the Program Joule I, contract JOUG-0009-C.

### Appendix A. 1D and 2D interpretation over a graben

The difference between the geometrical and electrical parameters of a complex structure, obtained from interpretations using 1D and 2D approaches, can be illustrated using a synthetic example. Data corresponding to a sounding (VES), made parallel to the strike direction, were generated using the model shown in Fig. 14 (top), which is a 2D generalized representation of the Chaves graben. These data were generated by a 2D program developed by Queralt et al. (1991). After the sounding data were generated, the apparent resistivity values were inputted into a 1D inversion program based on Johansen’s algorithm (Johansen, 1977). In the inversion procedure we resorted to the minimum number of layers required to fit the data. The high degree of misfit between the data and

model response (error about 12%), shows that the layered model is not able to represent properly the complete complex behavior originated by the 2D structure, mainly for  $AB/2$  in the range 680 to 1200 m. The calculated model is also shown in Fig. 14 (top). The estimated depth of the basement is 295 m and the resistivity of the conductive body is  $6 \Omega \text{ m}$ .

Based on the same model, a cross dipole–dipole line (dipole length of 300 m), was simulated. These dipole–dipole data were inverted using a 2D smoothness-constrained least-square algorithm (Sasaki, 1989). The obtained resistivity distribution, which fit the data to within 6% after four iterations, is shown in Fig. 14 (bottom). Although the 2D inversion method used in this investigation is unable to estimate a unique value of the depth of the basement, we can guess that it lies in the range of 500 to 750 m.

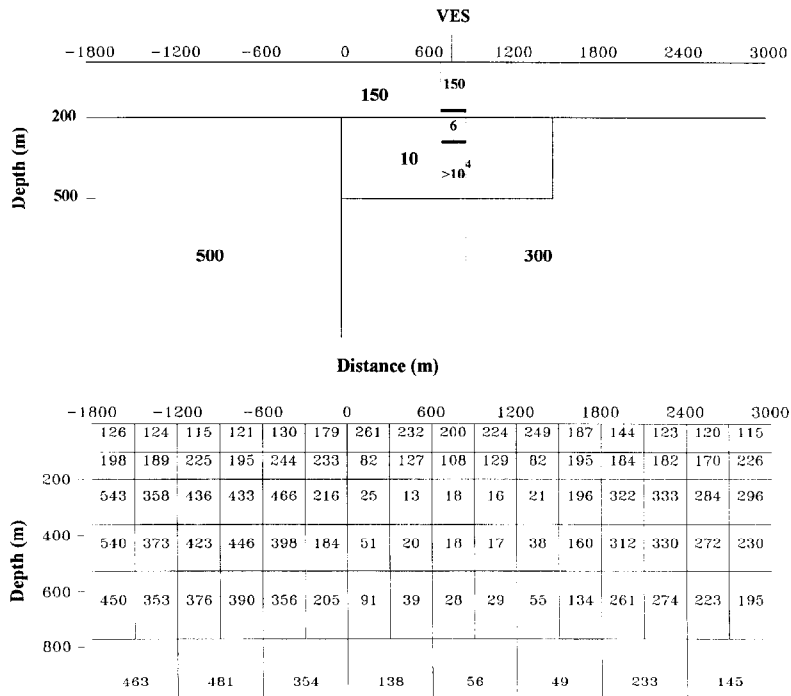


Fig. 14. Top: block geometries of the 2D test model and the 1D resistivity model obtained from 1D inversion of the VES sounding. Bottom: inversion result of the dipole–dipole synthetic data. The number in each block is the derived block resistivity in  $\Omega \text{ m}$ .

The main conclusions of this modeling exercise are as follows:

- the resistivity of the conductive zone is better estimated from parallel VES data;
- the depth of the basement is better estimated from dipole–dipole crossing data;
- the difference between the depth of the basement obtained by dipole–dipole and parallel VES can be high.

## References

- Aires-Barros, L., Graça, R.C., Marques, J.M., 1994. The low temperature geothermal system of Chaves (Northern Portugal): A geochemical approach. Proceedings of the Symposium Geothermics '94 in Europe, Doc. BRGM No. 203, pp. 67–73.
- Andrade Afonso, R.R., Monteiro Santos, F.A., Mendes Victor, L.A., 1994. The resistivity method in the evaluation of geothermal resources-application to Chaves (Portugal) geothermal field. Proceedings of the Symposium Geothermics '94 in Europe, Doc. BRGM No. 203, pp. 43–50.
- Bakbak, M.R., 1977. Three-dimensional modelling in resistivity and IP prospecting. Ph.D. Thesis, Univ. California.
- Campbell, D.L., 1977. Model for estimating electric macroanisotropy coefficient of aquifers with horizontal and vertical fractures. *Geophysics* 42 (1), 114–117.
- Dey, A., Morrison, H.F., 1979. Resistivity modelling for arbitrarily shaped three-dimensional bodies. *Geophysics* 44 (4), 753–780.
- Hidroprojecto, Acavaco, Tahal, 1987. Estudos das águas subterrâneas do vale de Chaves e seus vales secundários. Estudo realizado para a Direcção Regional de Agricultura de Trás-os-Montes. Lisboa.
- Johansen, H.K., 1977. A man/computer interpretation system for resistivity soundings over horizontally stratified earth. *Geophys. Prospect.* 25, 677–691.
- Monteiro Santos, F.A., Dupis, A., Andrade Afonso, A.R., Mendes-Victor, L.A., 1995a. Magnetotelluric observations over the Chaves geothermal field (NE Portugal): Preliminary results. *Phys. Earth Planet. Inter.* 91, 208–211.
- Monteiro Santos, F.A., Dupis, A., Andrade Afonso, A.R., Mendes-Victor, L.A., 1995b. Preliminary 3D modeling of the MT survey over Chaves Geothermal Field (NE Portugal). Proceedings of the International Symposium on Three-Dimensional Electromagnetics. Schlumberger-Doll Research, Ridgefield, USA, pp. 577–385.
- Monteiro Santos, F.A., Dupis, A., Andrade Afonso, A.R., Mendes-Victor, L.A., 1996. An audio-magnetotelluric survey over the Chaves geothermal field (NE Portugal). *Geothermics* 25 (3), 389–406.
- Poirmeur, C., Vasseur, G., 1988. Three-dimensional modeling of a hole-to-hole electrical method: Application to the interpretation of a field survey. *Geophysics* 53 (3), 402–414.
- Pridmore, D.S., 1978. Three-dimensional modeling of electrical and electromagnetic data using the finite element method. Ph.D. Thesis, University of Utah, 249 pp.
- Queralt, P., Pous, J., Marcuello, A., 1991. 2D resistivity modeling: An approach to arrays parallel to the strike direction. *Geophysics* 56 (7), 941–950.
- Raiche, A.P., 1974. An integral equation approach to three-dimensional modelling. *Geophys. J. R. Astr. Soc.* 36, 363–376.
- Sasaki, Y., 1989. Two-dimensional joint inversion of magnetotelluric and dipole–dipole resistivity data. *Geophysics* 54, 254–262.
- Scriba, H., 1981. Computation of the electric potential in the three-dimensional structures. *Geophys. Prospect.* 26, 790–802.
- Universidade de Trás-os-Montes e Alto Douro (UTAD), 1992. Evaluation of geothermal resources between Lamego e Vila Verde da Raia: Geological final report. Program JOULE/ECE-JOUG-0009-C.